0026-895X/11/7903-420–431$20.00
MOLECULAR PHARMACOLOGY
Copyright © 2011 The American Society for Pharmacology and Experimental Therapeutics
Mol Pharmacol 79:420–431, 2011

Vol. 79, No. 3
67959/3669932
Printed in U.S.A.

Functional and Biochemical Properties of Ryanodine Receptor Type 1 Channels from Heterozygous R163C Malignant Hyperthermia-Susceptible Mice

Wei Feng, Genaro C. Barrientos, Gennady Cherednichenko, Tianzhong Yang, Isela T. Padilla, Kim Truong, Paul D. Allen, José R. Lopez, and Isaac N. Pessah

Department of Molecular Biosciences, School of Veterinary Medicine, University of California, Davis, California (W.F., G.C.B., G.C., I.T.P., K.T., I.N.P.); and Department of Anesthesia, Perioperative and Pain Medicine, Brigham and Women's Hospital, Boston, Massachusetts (T.Y., J.R.L., P.D.A.)

Received August 1, 2010; accepted December 14, 2010

ABSTRACT

Mutations in ryanodine receptor type 1 (RyR1) confer malignant hyperthermia susceptibility. How inherent impairments in Ca^{2+} channel regulation affect skeletal muscle function in myotubes and adult fibers under basal (nontriggering) conditions are not understood. Myotubes, adult flexor digitorum brevis (FDB) fibers, and sarcoplasmic reticulum skeletal membranes were isolated from heterozygous knockin R163C and wild-type (WT) mice. Compared with WT myotubules, R163C myotubes have reduced Ca^{2+} transient amplitudes in response to electrical field pulses; however, R163C FDB fibers do not differ in their responses to electrical stimuli, despite heightened cellular cytoplasmic resting Ca^{2+} ($[Ca^{2+}]_{rest}$) and sensitivity to halothane. Immunoblotting of membranes from each genotype shows similar expression of RyR1, FK506 binding protein 12 kDa, and Ca^{2+}-ATPase, but RyR1 ^{2844}Ser phosphorylation in R163C muscle is 31% higher than that of WT muscle ($p < 0.001$). RyR1 channels reconstituted in planar lipid bilayers reveal ~65% of R163C channels exhibit ≥2-fold greater open probability (P_o) than WT, with prolonged mean open dwell times and shortened closed dwell times. [^{3}H]Ryanodine (Ry) binding and single-channel analyses show that R163C-RyR1 has altered regulation compared with WT: 1) 3-fold higher sensitivity to Ca^{2+} activation; 2) 2-fold greater [^{3}H]Ry receptor occupancy; 3) comparatively higher channel activity, even in reducing glutathione buffer; 4) enhanced RyR1 activity both at 25 and 37°C; and 5) elevated cytoplasmic $[Ca^{2+}]_{rest}$. R163C channels are inherently more active than WT channels, a functional impairment that cannot be reversed by dephosphorylation with protein phosphatase. Dysregulated R163C channels produce a more overt phenotype in myotubes than in adult fibers in the absence of triggering agents, suggesting tighter negative regulation of R163C-RyR1 within the Ca^{2+} release unit of adult fibers.

Introduction

Human malignant hyperthermia (MH)-susceptible patients remain subclinical until challenged with one or more pharmacological triggering agents, including halogenated volatile anesthetics and depolarizing neuromuscular blockers (Zhou et al., 2010). A fulminant MH episode during the perioperative period is often lethal if not promptly treated with dantrolene. When a familial history of MH is suspected (Lehmann-Horn et al., 2008), MH susceptibility (MHS) is typically diagnosed with an in vitro contracture test. Although in vitro contracture test testing is a good prognosticator of MH, fatal cases continue to occur annually in the United States and throughout the world (Zhou et al., 2010). MHS is an inherited autosomal dominant muscle disorder with a heterogeneous etiology. Common to all fulminant MH episodes is a severe defect in skeletal muscle Ca^{2+} regulation that is not evident (remains subclinical) in the absence of an environmental trigger. More than 50% of the families with a familial history of MHS have linkage to one of >175 mutations within RYR1 located on 19q13.1, the gene that encodes

This work was supported by the National Institutes of Health National Institute of Arthritis and Musculoskeletal and Skin Disease [Grants AR46513, AR52354]; and the National Institute of Environmental Health Sciences [Grants ES014901, ES04699].
W.F. and G.C.B. contributed equally to this work.
Article, publication date, and citation information can be found at http://molpharm.aspetjournals.org.
doi:10.1124/mol.110.067959.

ABBREVIATIONS: MH, malignant hyperthermia; MHS, malignant hyperthermia susceptibility; RyR1, ryanodine receptor type 1; SR, sarcoplasmic reticulum; EC, excitation-contraction; $[Ca^{2+}]_{rest}$, cellular cytoplasmic resting Ca^{2+}; DHPR, dihydropyridine receptor; CRU, Ca^{2+} release unit; WT, wild type; ECCE, excitation-coupled calcium entry; FDB, flexor digitorum brevis; *F*, fluorescence; PAGE, polyacrylamide gel electrophoresis; SERCA, sarcoplasmic reticulum/endoplasmic reticulum calcium ATPase; FKBP12, FK506 binding protein 12 kDa; PP1, protein phosphatase 1; Ry, ryanodine; TG, thapsigargin; GSH, glutathione; GSSH, oxidized glutathione; BLM, bilayer lipid membrane; P-, phosphorylated.

the skeletal isoform of ryanodine receptor type 1 (RyR1) (Robinson et al., 2006). RyR1 is responsible for releasing ionized calcium (Ca^{2+}) from SR stores during excitation-contraction (EC) coupling and is essential for muscle contraction (Takeshima et al., 1994; Buck et al., 1997). Of the additional loci linked to MHS, one within the *CACNA1S* gene encodes for the pore-forming subunit of the L-type voltage-dependent Ca^{2+} channel $Ca_v1.1$ localized within T-tubule membranes (also termed DHPR) (Robinson et al., 2003). The DHPR is responsible for RyR1 activation during EC coupling, an essential step for triggering muscle contraction. RyR1 and its protein-binding partners assemble a tightly regulated macromolecular complex within the T-tubule-SR junctions termed "Ca^{2+} release units" (CRUs). A prominent feature of the CRU is a physical interaction between the DHPR and RyR1 that permits precise alignment of DHPR tetrads over every other RyR1 (Protasi, 2002), an arrangement that is essential for engaging bidirectional signaling between the DHPR and RyR1. Thus, the ultrastructural organization of the CRU proteins is tightly linked to precise positive and negative regulation between DHPR and RyR1 Ca^{2+} channels (Sheridan et al., 2006).

Recent studies have shown that MHS mutations alter bidirectional signaling between DHPR and RyR1 even in the absence of triggering agents (Bannister et al., 2010). Thus, Ca^{2+} dysregulation in skeletal muscle does not only manifest during the acute period of a triggered MH episode. Chronic elevation of Ca^{2+} in the myoplasm of resting muscle cells ($[Ca^{2+}]_{rest}$) is a common feature of skeletal muscle expressing MHS mutations (Yang et al., 2007a). In this respect, expression of normal RyR1 channels seems to critically regulate $[Ca^{2+}]_{rest}$ in skeletal myotubes by contributing Ca^{2+} leak from SR and causing increased Ca^{2+} entry (Eltit et al., 2010). Thus, altered DHPR-RyR1 bidirectional signaling and elevated $[Ca^{2+}]_{rest}$ may confer MHS.

Heterozygosis for R163C-RyR1 (R163C) is one of the five most common mutations conferring MHS in humans (Robinson et al., 2006). A knockin mouse model of R163C was generated and shown to possess the hallmarks of MHS (Yang et al., 2006). Although R163C homozygous mice are not viable at birth, mice heterozygous for the mutation (referred to as R163C mice here) model the human condition in that they exhibit no overt clinical phenotype until they are challenged with either heat stress or a general anesthetic (e.g., halothane), which triggers a fulminant MH episode. Myotubes isolated from R163C MHS mice also show significant deviations from wild-type (WT) myotubes in the absence of triggering agents, including 1) elevated $[Ca^{2+}]_{rest}$ (Yang et al., 2007b); 2) enhanced excitation-coupled Ca^{2+} entry (ECCE) (Cherednichenko et al., 2008); 3) altered retrograde signaling to the DHPR, resulting in a shift of SR Ca^{2+} release to more hyperpolarized potentials and a concomitant decrease in the transient amplitude ($\Delta F/F_0$) (Bannister et al., 2010); and 4) higher sensitivity of R163C expressing myotubes to stimulation by pharmacological and physiological ligands such as caffeine, 4-chloro-*m*-cresol, and K^+-induced depolarization than WT (Estève et al., 2010). The present study identifies fundamental biochemical and functional impairments inherent in R163C channels isolated from R163C heterozygous mice. Dysregulated R163C channels produce a more overt phenotype in cultured myotubes than in adult fibers in the absence of a triggering agent, providing the first evidence of tighter negative regulation of R163C in adult fibers, possibly conferred by DHPR.

Materials and Methods

Animal Use

All collection of mouse tissues was conducted using protocols approved by the Institutional Animal Care and Use Committees at the University of California (Davis, CA) and Department of Anesthesia, Perioperative and Pain Medicine, Brigham and Women's Hospital (Boston, MA).

Preparation of Primary Myotubes and Adult FDB Fibers

Primary skeletal myoblast lines were isolated from 1- to 2-day-old C57/BL6 WT mice and from newborn mice heterozygous for mutation R163C MH, as described previously (Cherednichenko et al., 2004). The myoblasts were expanded in 10-cm cell culture-treated Corning dishes coated with collagen (Calbiochem, San Diego, CA) and were plated onto 96-well μ-Clear plates (Greiner Bio-One, Longwood, FL) coated with Matrigel (BD Biosciences, San Jose, CA) for Ca^{2+} imaging studies. Upon reaching ~80% confluence, growth factors were withdrawn, and the cells were allowed to differentiate into myotubes over a period of 3 days.

Flexor digitorum brevis (FDB) were dissected from 3- to 6-month-old WT and R163C heterozygous mice, and single intact myofibers were enzymatically isolated as described previously (Brown et al., 2007). To reduce stress-activated SR Ca^{2+} release during isolation, especially in R163C fibers, 10 μM dantrolene was included in the initial dissociation medium. After isolation, the fibers were plated on Matrigel-coated plates (BD Biosciences) and maintained in Dulbecco's modified Eagle's medium (Invitrogen, Carlsbad, CA) supplemented with 10% fetal bovine serum (Thermo Fisher Scientific, Waltham, MA) and 0.1 mg/ml penicillin-streptomycin (Sigma Aldrich, St. Louis, MO) in the absence of dantrolene. Fibers were kept overnight in a 5% CO_2 incubator, and experiments were conducted within 12 to 24 h after plating.

Measurements of Ca^{2+} Transients

Myotubes were loaded with the Ca^{2+} indicator Fluo-4-acetoxymethyl ester (Invitrogen) at 37°C for 20 min in imaging buffer composed of 125 mM NaCl, 5 mM KCl, 2 mM $CaCl_2$, 1.2 mM $MgSO_4$, 6 mM dextrose, and 25 mM HEPES, pH 7.4, supplemented with 0.05% bovine serum albumin. Myotubes were then washed three times with imaging buffer and transferred to the stage of a Diaphot inverted microscope (Nikon, Tokyo, Japan) and illuminated at the isosbestic wavelength for Fura-2 or at 494 nm for Fluo-4 with a DeltaRam excitation source (Photon Technology International, Lawrenceville, NJ). Fluorescence emission at 510 nm was captured from regions of interest within each myotube from three to 10 individual cells at six frames per second by using a 40×, 1.3 numerical aperture objective (Nikon), IC-300 intensified charge-coupled device camera, and images were digitized and analyzed with ImageMaster software (Photon Technology International). Electrical field stimuli were applied using two platinum electrodes fixed to opposite sides of the well and connected to an A.M.P.I. Master 8 stimulator (A.M.P.I., Jerusalem, Israel) set at 7-V, 0.5-ms bipolar total pulse duration, over a range of frequencies (2–60 Hz; 10-s pulse train duration; 30-s rest between pulse trains). Transient amplitude was measured by normalizing peak change in Fluo-4 fluorescence (ΔF) to the florescence baseline (F_0) and is presented as mean $\Delta F/F_0$ for each myotube included in the analysis. The means ± S.E.M. were calculated from the number of cells indicated in the figure legends and were obtained from at least two different experimental days. Statistical analysis was performed with one-way analysis of variance.

FDB fibers were loaded with Fluo-4 acetoxymethyl ester (10 μM; 40 min at room temperature) in normal Ringer's solution containing146 mM NaCl, 4.7 mM KCl, 0.6 mM $MgSO_4$, 6 mM glucose, 25

mM HEPES, 2 mM $CaCl_2$, and 0.02% Pluronic F127 (Invitrogen). The cells were then washed three times with Ringer's and transferred to the stage of an IX71 inverted microscope equipped with a 40 × 0.9 numerical aperture objective (Olympus, Center Valley, PA) and illuminated at 494 nm to excite Fluo-4 with a DeltaRam wavelength-selectable light source (Photon Technology International). The contractility inhibitor *N*-benzyl-*p*-toluene sulfonamide (20 μM) was added to the imaging buffer before initiating measurement to prevent movement artifacts. Fluorescence emission at 510 nm was captured from individual fibers. Electrical field stimuli were applied using two platinum electrodes fixed to opposite sides of the well and connected to an A.M.P.I. Master 8 stimulator set at 4-V, 0.5-ms bipolar pulse duration over a range of frequencies (1–20 Hz; 10-s pulse train duration). Halothane was dissolved in Ringer's solution, and the concentration was confirmed by mass spectrometry. The FDB fibers were perfused with 0.1% halothane prepared just before needed. Fluo-4 fluorescence emission was measured at 30 frames/s by using a Cascade 512B camera (Photometrics, Tucson, AZ). The images were acquired using the Easy Ratio Pro software (Photon Technology International). The data were analyzed using Origin 7 software (OriginLab Corp., Northampton, MA). Transients were normalized to the F_0 of each individual fiber, and the mean integrated area within the evoked responses was calculated from the number of fibers indicated in the figure legends. Statistical comparisons were performed with an unpaired Student's *t* test.

Determination of $[Ca^{2+}]_{rest}$

Ca^{2+}-Selective Microelectrodes. Double-barreled Ca^{2+}-selective microelectrodes were prepared and calibrated as described previously (Eltit et al., 2010). Only those electrodes with a linear relationship between pCa3 and pCa8 (Nernstian response, 28.5 mV/pCa unit at 24°C) were used experimentally. To better mimic the intracellular ionic conditions, all calibration solutions were supplemented with 1 mM Mg^{2+}. All electrodes were then recalibrated after making measurements of $[Ca^{2+}]_{rest}$, and if the two calibration curves did not agree within 3 mV from pCa7 to pCa8, the data from that microelectrode were discarded.

Recording of V_m and $[Ca^{2+}]_{rest}$. Measurements were performed on two preparations: cultured myotubes and mice sedated with nontriggering ketamine/xylazine (100/5 mg/kg). Once mice were fully anesthetized (lack of tail-pinch response), small incisions were made to expose the vastus lateralis muscle of each leg, and the fibers were impaled with the double-barreled microelectrode. Potentials were recorded via an FD-223 high-impedance amplifier (WPI, Sarasota, FL). The potential from the 3 M KCl barrel (V_m) was subtracted electronically from VCa_E, to produce a differential Ca^{2+}-specific potential (V_{Ca}) that represents the $[Ca^{2+}]_{rest}$. V_m and V_{Ca} were filtered (30–50 kHz) to improve the signal-to-noise ratio and stored in a computer for further analysis.

Isolation of Membrane Fractions from Mouse Skeletal Muscle

Skeletal muscles collected from either WT or heterozygous R163C knockin mice (one to three animals/preparation; 3–6 months old) were minced on ice; placed in ice-cold buffer containing 200 mM sucrose, 5 mM imidazole, 0.01 mM phenylmethylsulfonyl fluoride, and 5 μg/ml leupeptin, pH 7.4; and homogenized with three sequential bursts (30 s each) of a PowerGen 700D homogenizer (Thermo Fisher Scientific) at 9000, 18,000, and 18,000 rpm. Homogenates were centrifuged at 10,000*g* for 20 min. Supernatants were saved, and the pellets were subjected to a second round of homogenization and centrifugation at the same settings as mentioned above. The remaining pellets were discarded, and the supernatants were combined and poured through four layers of cheesecloth. The filtrate was centrifuged at 110,000*g* for 60 min at 4°C. Pellets were resuspended in 200 mM sucrose and 10 mM HEPES, pH 7.4; aliquoted into microfuge tubes (100 μl/sample); and either stored at −80°C for biochemical analyses or subjected to further purification to obtain membranes enriched in junctional SR. Protein concentration for each preparation was determined using the DC Protein Assay kit (Bio-Rad Laboratories, Hercules, CA).

Western Blotting

Skeletal muscle membrane preparations were denatured in SDS-PAGE sample buffer (Bio-Rad Laboratories) containing 2.5% 2-mercaptoethanol at 60°C for 5 min. Protein (10 or15 μg/lane) was loaded onto Tris-acetate 4-to-12% or 4-to-20% acrylamide gradient SDS-PAGE gels (Invitrogen), electrophoresed at 150 V for 75 min (4°C), and then transferred to polyvinylidene difluoride membranes at 30 V for 15 h and then at 110 V for another 1 h (4°C). Membranes were blocked with Odyssey blocking buffer (LI-COR Biosciences, Lincoln, NE) for 30 min and incubated overnight at 4°C with the primary antibodies. Total RyR1 was detected with antibody 34C (Airey et al., 1990) at 1:1000 dilution (Developmental Studies Hybridoma Bank, University of Iowa, Iowa City, IA). Phospho-epitope-specific antibody that recognizes mouse RyR1 ^{2844}Ser, a protein kinase A phosphorylation site (Reiken et al., 2003), was purchased from Abcam Inc. (Cambridge, MA) and used at 1:2000 dilution. SR/endoplasmic reticulum Ca^{2+}-ATPase was detected using a SERCA1-selective monoclonal (Pierce Chemical, Rockford, IL) diluted to 1:5000 or 1:20,000. FKBP12 was detected using a commercial polyclonal antibody (Pierce Chemical) diluted 1:2500. After incubation with primary antibody, each polyvinylidene difluoride membrane was washed five times (5 min each) with phosphate-buffered saline containing 0.1% Tween 20 and incubated with infrared fluorescent-conjugated secondary antibodies diluted to 1:10,000; 800 nm fluorescent-conjugated goat anti-mouse (LI-COR Biosciences), and 700 nm fluorescent-conjugated goat anti-rabbit (LI-COR Biosciences). The membranes were washed five times with 0.1% Tween 20/phosphate-buffered saline and scanned with an Odyssey infrared imager (LI-COR Biosciences); band intensity was analyzed using Odyssey version 3.0 software (LI-COR Biosciences). Signals from each Western blot were analyzed for 1) total R163C protein (green channel) normalized to the WT-RyR1 signal on the same blot (each run in duplicate lanes) and 2) the ratio of the phospho-^{2844}Ser signal (red channel) to its respective green channel. In total, $n = 29$ separate blots from five paired R163C and WT skeletal muscle preparations were analyzed. FKBP12 expression was analyzed from $n = 2$ paired R163C and WT preparations; total blots, $n = 10$ from R163C; $n = 8$ from WT. SERCA expression was analyzed from a total of $n = 3$ paired R163C and WT preparations, each run in duplicate lanes and normalized to the WT signal.

Dephosphorylation of R163C-RyR1 and WT RyR1 by Protein Phosphatase 1

Protein phosphatase 1 (PP1; New England Biolabs, Ipswich, MA) was used to dephosphorylate SR protein according to the vendor's instructions. The reaction mixture contained 50 mM HEPES, 100 mM NaCl, 2 mM dithiothreitol, 1 mM $MnCl_2$, 0.01% Brij 35, pH 7.5, 4 mg/ml SR protein (R163C or WT), and 200 units/ml PP1, and the mixture was incubated at 30°C for 10 min. Then, the samples were diluted into SDS-PAGE sample buffer for Western blotting or into [^{3}H]ryanodine binding buffer (see below).

Measurements of [^{3}H]Ryanodine Binding to RyR1

The apparent association or equilibrium binding of [^{3}H]ryanodine ([^{3}H]Ry) to RyR1 was measured at 25 or 37°C for 0 to 3 h with constant shaking in buffer consisting of 100 to 150 μg of protein/ml, 2 to 5 nM [^{3}H]Ry (PerkinElmer Life and Analytical Sciences, Boston, MA), 250 mM KCl, and 20 mM HEPES. RyR1 channel modulators Ca^{2+}, Mg^{2+}, and/or glutathione were titrated in specific experiments as described in the figure legends. Nonspecific [^{3}H]Ry binding was determined in the presence of 1000-fold excess unlabeled ryanodine. Bound and free ligand were separated by rapid filtration through

Whatman GF/B glass fiber (Whatman, Clifton, NJ) filters using a Brandel cell harvester (Brandel Inc., Gaithersburg, MD) with 5 ml of ice-cold buffer (250 mM KCl, 20 mM HEPES, 15 mM NaCl, and 50 μM Ca^{2+}, pH 7.4). [^{3}H]Ry retained in filters were quantified by liquid scintillation spectrometry using a scintillation counter (model 6500; Beckman Coulter, Fullerton, CA). Each experiment was performed on at least three independent skeletal muscle preparations, each in triplicate. Linear or nonlinear curve-fitting was performed using Origin software (OrginLab Corp.).

Measurement of SERCA Activity

Activity of the thapsigargin (TG)-sensitive Ca^{2+}-ATPase (SERCA1) was measured in the same skeletal membrane preparations used for Western blotting and receptor binding analyses using a coupled enzyme assay that monitors the rate of oxidation of NADH at 340 nm, as described previously (Ta et al., 2006). In brief, 1.5 ml of assay buffer consisted of 7 mM HEPES, pH 7.0, 143 mM KCl, 7 mM $MgCl_2$, 0.085 mM EGTA, 0.43 mM sucrose, 0.0028 mM phosphoenolpyruvate, 1 mM Na_2ATP, coupling enzyme mixture (700 units of pyruvate kinase II and 1000 units of lactate dehydrogenase), 0.048 mM free Ca^{2+}, and 50 μg/ml protein at 37°C. TG (0.2 μM) was added to inhibit the SERCA1 component of ATPase activity (negative control). NADH (0.4 mM) was added to initiate measurement of Ca^{2+} (Mg^{2+}) ATPase activity. In total, six measurements were made from at least two paired R163C and WT preparations.

Glutathione Stock Solutions and Redox Potential Calculations

GSH was dissolved in degassed 10 mM HEPES buffer, and the solution was adjusted to pH 7.0. Aliquots (~0.5 ml) were transferred to vials and sealed after blowing with argon. The vials were stored at −20°C for less than a month. Once thawed and opened for use, the vial was discarded. Oxidized glutathione (GSSG) solution also was made and stored in a similar manner, except without degassing and argon protection. Redox potentials were calculated according to the Nernst equation, $E_h = E_o + RT/2F \ln [(GSSG)/(GSH)^2]$, where E_o is the standard state redox potential of glutathione at −240 mV (Hwang et al., 1995).

Single-Channel Measurements in BLM

Planar lipid bilayer was formed by phosphatidylethanolamine/phosphatidyl-serine/phosphatidylcholine [5:3:2 (w/w); Avanti Polar Lipids, Alabaster, AL]. Chambers defined as *cis* and *trans* contained a 10-fold Cs^+ gradient (500:50), where *cis* was virtually grounded. Proteins, Ca^{2+}/EGTA, and/or Na_2ATP was added to the *cis* chamber. Transmembrane redox potentials were instilled by adding defined [GSH]/[GSSH] at on *cis* and *trans* chambers, respectively. Both *cis* and *trans* chambers were buffered to pH 7.4 with 10 mM HEPES. Single-channel activity was measured using a patch-clamp amplifier (bilayer clamp BC 525C; Warner Instruments, Hamden, CT) at a holding potential of −40 mV applied to the *trans* chamber. The amplified current signals, filtered at 1 kHz (low-pass Bessel filter 8 pole; Warner Instruments), were digitized and acquired at a sampling rate of 10 kHz (Digidata 1320A; Molecular Devices, Sunnyvale, CA). All current recordings were made with Axoscope 10 software (Molecular Devices) for at least 1 min under each experimental condition. The channel open probability (P_o), mean open times, and mean closed dwell times (t_o and t_c) were calculated using Clampfit, pClamp software 9.0 (Molecular Devices). The number of channels recorded under each *cis*/*trans* condition is specified in the respective figure legends. Differences in R163C and WT P_o were tested for statistical significance using unpaired Student's *t* tests.

Results

Altered Ca^{2+} Transient Properties of Skeletal Myotubes, but Not FDB Fibers, Isolated from R163C Heterozygous Mice. Primary myotubes cultured from WT and R163C heterozygous mice were challenged with electrical pulses ranging from 2 to 60 Hz at 25°C. Although both genotypes responded in a robust manner to electrical pulses, the amplitude of the Ca^{2+} transients were consistently lower in R163C myotubes compared with WT myotubes across the entire frequency range tested ($p < 0.01$; Fig. 1, A and B). We reported previously that R163C myotubes exhibit a significantly higher rate of Mn^{2+} entry than WT myotubes during stimulation with a 20-Hz pulse train, and this has been ascribed to enhanced ECCE in the mutant (Cherednichenko et al., 2008). Here, we tested the magnitude of ECCE across a broad range of stimulus frequencies. R163C myotubes show significantly higher rates of ECCE between 2 and 20 Hz compared with the WT ($p < 0.005$; Fig. 1C). However, with

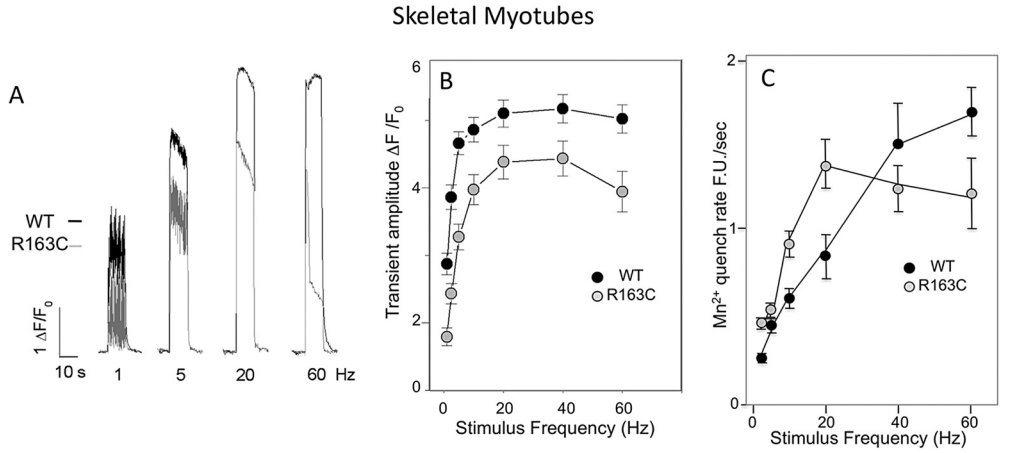

Fig. 1. Myotubes isolated for R163C heterozygous and WT mice differ in their responses to electrical stimuli. A, skeletal myotubes were stimulated by electrical field at 1 to 60 Hz and Ca^{2+} transients measured with Fluo-4 monitored at 25°C as described under *Materials and Methods*. Shown are representative responses to 1, 5, 20, and 60 Hz from WT (black trace) and R163C myotubes (gray trace). B, summary data showing mean ± S.E.M. of normalized Ca^{2+} transient amplitudes for WT ($n = 21$ cells) and R163C ($n = 24$ cells) measured from at least three different cultures. The transient amplitude elicited in R163C myotubes was significantly lower than WT at all stimulation frequencies ($p < 0.01$). C, electrically evoked Mn^{2+} entry was measured during field stimulation at 2 to 60 Hz by using the quench of Fura-2 fluorescence as described under *Materials and Methods*. The rate of Mn^{2+} entry was significantly greater in R163C compared with WT myotubes with 2-, 10-, 20-, 40-, and 60-Hz stimuli ($p < 0.01$), whereas the rate of Mn^{2+} quench was significantly lower in R163C compared with WT with a 60-Hz stimulus ($p < 0.005$). Data shown are means ± S.E.M. from n = 8 to 29 myotubes measured at each frequency.

stimuli >20 Hz, R163C myotubes show a tendency for ECCE to plateau or decrease, whereas in WT myotubes ECCE increases throughout the stimulus range tested (i.e., the rate of Mn^{2+} entry increases with stimulus frequency between 2 and 60 Hz). In this regard, WT myotubes attain significantly higher rates of ECCE than R163C myotubes at 60 Hz ($p < 0.005$; Fig. 1C).

In contrast to results obtained with myotubes, differences in the magnitude of electrically evoked Ca^{2+} transients did not differ between WT and R163C adult FDB fibers in the range of 1 to 20 Hz, when measured under the same experimental conditions (Fig. 2, A and B). As expected, FDB fibers isolated from R163C heterozygous mice exhibited a significantly amplified response to halothane challenge compared with WT under these experimental conditions, unmasking their MHS properties (Fig. 2, C and D).

Elevated $[Ca^{2+}]_{rest}$ in R163C Myotubes and In Vivo Adult Fibers. Microelectrode measurements showed that heterozygous R163C myotubes in culture have ~2.2-fold chronically elevated $[Ca^{2+}]_{rest}$ compared with their WT counterparts (Fig. 3). Likewise, in vivo measurements of $[Ca^{2+}]_{rest}$ in the vastus lateralis of ketamine/xylazine-anesthetized mice showed ~2.7-fold higher $[Ca^{2+}]_{rest}$ in R163C compared with $[Ca^{2+}]_{rest}$ in WT fibers (Fig. 3).

RyR1, P-^{2844}Ser-RyR1, FKBP12, and SERCA Expression. Skeletal muscle membranes prepared from R163C knockin and WT mice under basal (nontriggered) conditions were evaluated for the level of expression of RyR1 protein and its level of phosphorylation at ^{2844}Ser (P-^{2844}Ser). Figure 4A shows results from a typical Western blot probed with monoclonal antibody 34C that recognizes RyR1, indicating no significant differences were detected in the level of RyR1 protein expression between the two genotypes (Fig. 4A, green channel; Fig. 4B, summary data from $n = 29$ blots from five paired preparations). However, the same blots probed with an antibody that recognizes phosphorylation at ^{2844}Ser (P-^{2844}Ser-RyR1) showed a consistently significantly higher signal with preparations obtained from heterozygous R163C compared with WT mice (Fig. 4A, red channel). Quantitative analyses of the green and red channels by imager analyses (LI-COR Biosciences) identified 30.8% higher ratios of P-^{2844}Ser-RyR1/total RyR1 in R163C preparations compared with those from WT (Fig. 4C; $p < 0.001$).

In separate Western blot experiments, the antibody that recognizes RyR1 was used in combination with an antibody that recognizes FKBP12 or SERCA1, respectively. The results showed that the ratio of total RyR1/FKBP12 immunoreactive protein was not significantly different between ge-

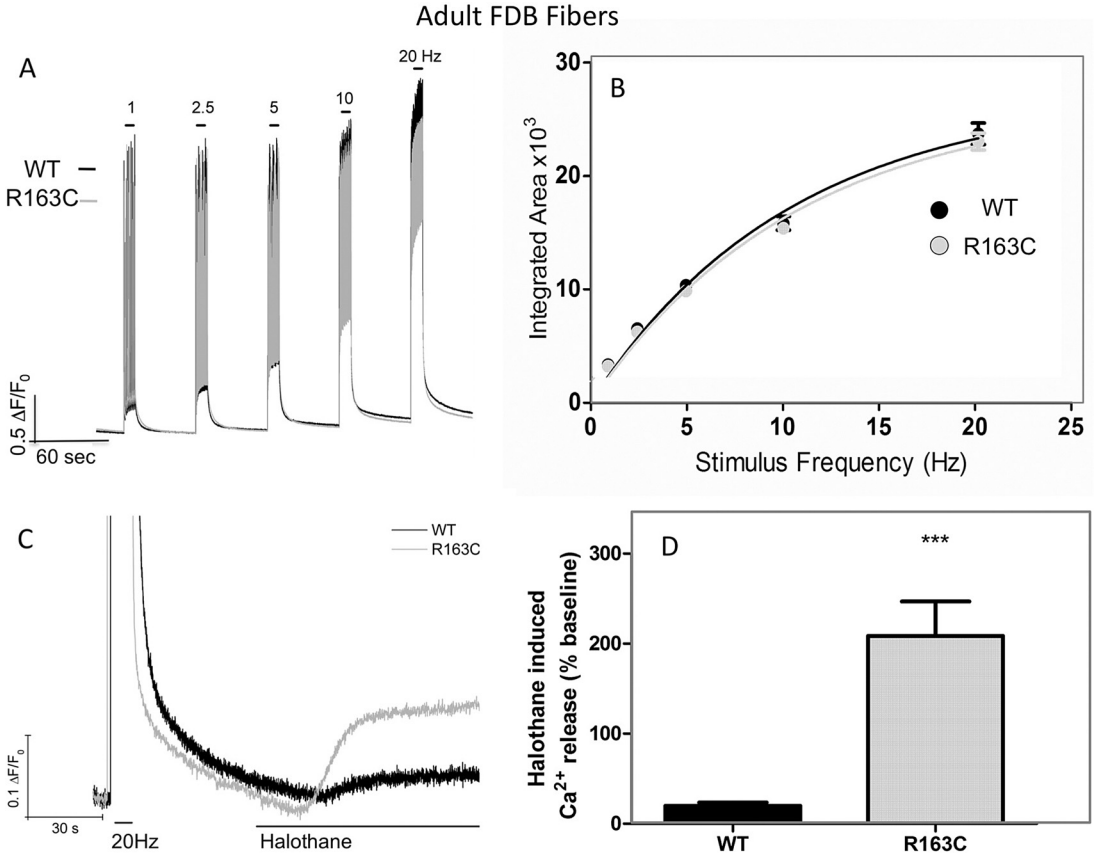

Fig. 2. Adult FDB fibers isolated for R163C heterozygous MHS and WT mice do not differ in their responses to electrical stimuli. A, representative traces showing the frequency responses in WT (black traces) and R163C (gray traces) FDB fibers. Fibers were loaded with Fluo-4, and Ca^{2+} responses were elicited by electric field stimulation at 1, 2.5, 5, 10, and 20 Hz (10-s duration) as described under *Materials and Methods*. B, for each stimuli frequency, the integrated area was calculated and plotted as mean ± S.E.M. WT ($n = 68$) from four different fiber isolations and R163C ($n = 78$) from two different fiber isolations. C, representative trace showing that FDB fibers isolated from R163C show an amplified response to acute challenge with 0.1% halothane in the perfusion medium compared with FDB isolated from WT mice. D, amplitude of the Ca^{2+} response 30 s after the start of perfusion with halothane (0.1%). The magnitude of halothane-induced Ca^{2+} release was normalized to the baseline of each fiber 10 s before commencing perfusion of halothane. The data shown are mean ± S.E.M. obtained from $n = 16$ R163C and $n = 24$ WT fibers from two separate isolations (***, $p < 0.001$).

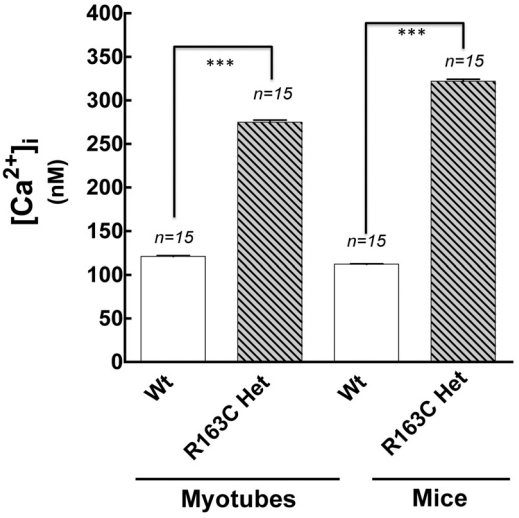

Fig. 3. Elevated $[Ca^{2+}]_{rest}$ in heterozygous (Het) R163C myotubes and adult fibers. Microelectrode measurements of $[Ca^{2+}]_{rest}$ in cultured myotubes and in adult vastus lateralis fibers in vivo were made as described under *Materials and Methods*. The data shown are mean ± S.E.M. $[Ca^{2+}]_{rest}$ values, which differed significantly between WT and R163C for both cultured myotubes and adult fibers (***, $p < 0.001$).

notypes, either in the level of FKBP12 (Fig. 4, D and E) or SERCA1 (Fig. 4, F and G) protein expression. Moreover, neither TG-sensitive Ca^{2+} ATPase activity (Fig. 4H) nor the ratio of total RyR1/SERCA1 immunoreactive protein (data not shown) exhibited detectable differences between the two genotypes. Collectively, these data suggested that although total RyR1, FKBP12, and SERCA1 protein expressions were not significantly altered in R163C-RyR1 skeletal muscle, significantly elevated P-^{2844}Ser-RyR1 expression was detected in R163C compared with WT.

RyR1-R163C Channels Have Inherently Higher Open Probability Than WT. R163C- or WT-RyR1 channels were incorporated into BLM by induced fusion of SR vesicles. In the presence of 1 mM free cytosolic (*cis*) Ca^{2+}, 2 mM Na_2ATP, and 100 μM free luminal (*trans*) Ca^{2+}, the single-channel activity was recorded at a holding potential of −40 mV (applied to *trans*). Figure 5A, top, shows representative current traces from a WT channel. Under these *cis*/*trans* conditions, the typical mean P_o of WT channels was 0.149 ± 0.034 ($n = 9$). In contrast, $n = 23$ independent reconstitutions in total of channels prepared from heterozygous R163C mouse skeletal muscle exhibited a significantly wider divergence of P_o values compared with

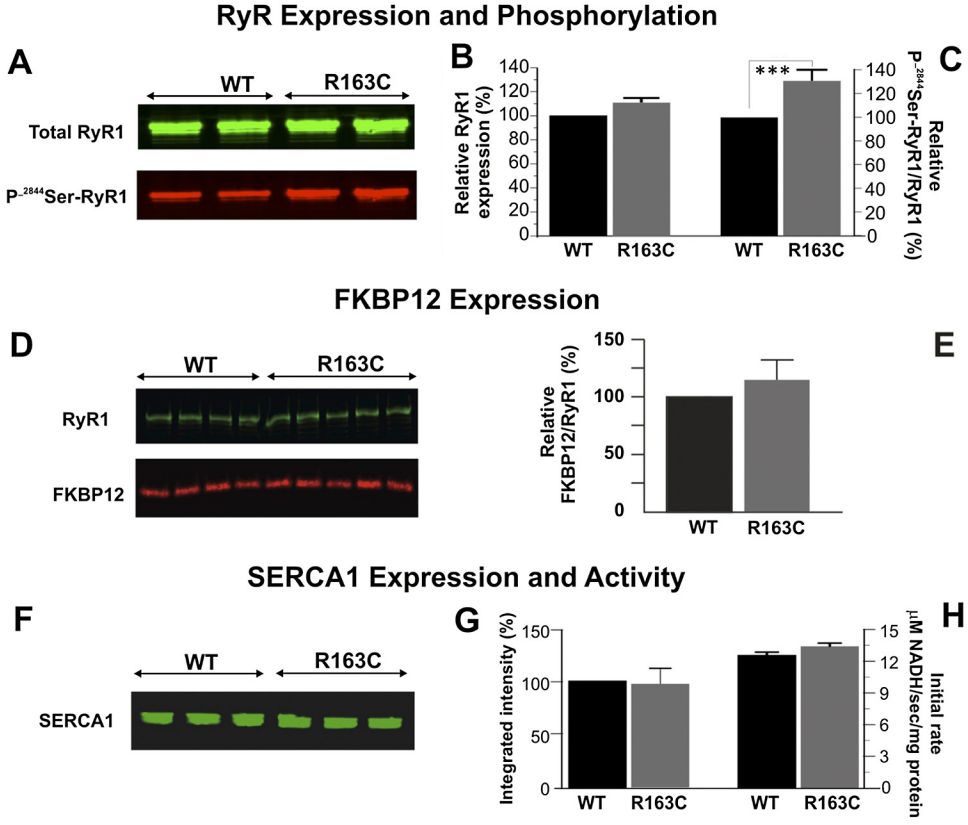

Fig. 4. No differences in total RyR1, FKBP12, and SERCA expression were noted, but we observed enhanced phosphorylation of ^{2844}Ser-RyR1 in preparations from R163C heterozygous compared with those from WT mice. A, representative Western blot from five independent preparations showing the expression of RyR1 probed with monoclonal 34C (total RyR1, green channel) and an antibody that selectively recognizes phosphorylated ^{2844}Ser-RyR1 (P-^{2844}Ser-RyR1, red channel). B, densitometry results show no differences between R163C and WT for total RyR1 protein expression. Bar graph represents the mean ± S.E.M. for $n = 21$ blots from seven membrane preparations. C, densitometry results show that R163C has significantly higher levels of P-^{2844}Ser-RyR1 compared with WT. P-^{2844}Ser-RyR1 signal (red channel) was normalized to total RyR1 (green channel) for each Western blot. The bar graph represents the mean ± S.E.M. for $n = 29$ blots from five membrane preparations. D, representative Western blot showing RyR1 (green channel) and FKBP12 (red channel). E, mean ± S.D. densitometry results from WT ($n = 8$) and R163C ($n = 10$) of two paired protein preparations. F, representative Western blot showing the SERCA1 expression from three separate preparations from WT and R163C mice. For each sample, 5 μg of protein was loaded per lane. G, mean ± S.E.M. densitometry results from $n = 4$ preparations per genotype replicated in triplicate. H, mean ± S.E.M. of the Ca^{2+}-ATPase activity measured in an assay that couples Ca^{2+}-dependent ATP hydrolysis to NADH oxidation (coupled enzyme assay) as described under *Materials and Methods*. The initial rate of NADH oxidation are shown for $n = 6$ determinations for WT and R163C. Specificity was assessed via TG; >95% of the initial rate of NADH oxidation was TG-sensitive.

WT. Successful reconstitutions from R163C membranes produced a frequency of channels that gated with significantly higher P_o than those reconstituted from WT (Fig. 5A, bottom traces). Of the 23 R163C channels recorded, 13.0% exhibited P_o values that were ~2-fold higher than the mean P_o measured with WT channels, 30.4% exhibited P_o values that were 2- to 4-fold higher than WT, and 21.7% exhibited >4-fold higher P_o values than WT (Fig. 5B). In contrast, 34.8% of the R163C channels exhibited P_o values that were not statistically different ($p > 0.05$) from the mean behavior of channels reconstituted from WT (Fig. 5B).

Dephosphorylation of RyR1-R163c Has No Significant Effect on Channel Activity. The inherently higher P_o of R163C-RyR1 channels may be a consequence of the increased phosphorylation compared with WT channels. This hypothesis was directly tested by pretreatment of R163C and WT SR membranes with PP1 (see *Materials and Methods*). Western blotting of total RyR1 and P-^{2844}Ser-RyR1 showed near-complete dephosphorylation was achieved by PP1 pretreatment in both genotypes, whereas sham incubations lacking PP1 preserved P-^{2844}Ser-RyR1 and the higher level of phosphorylation in R163C preparations (Fig. 6A). The functional consequence of dephosphorylation was analyzed using [^{3}H]Ry binding analysis. Figure 6B shows that there are negligible differences between PP1-pretreated and sham-treated membrane preparations from either genotype, suggesting that phosphorylation and dephosphorylation had no significant effect on RyR1 channel activity.

[^{3}H]Ry Binding and Regulation by Ca^{2+} Is Altered by the R163C Mutation. Ca^{2+} is a physiological modulator of RyR1 channel activity. Ca^{2+} enhances [^{3}H]Ry binding by interactions with high-affinity activation sites and inhibits the channel by interaction with allosterically coupled low-affinity sites, and it facilitates removal of the inherent Mg^{2+} block (Voss et al., 2008). We examined whether preparations from R163C differed from those of the WT in their ability to bind [^{3}H]Ry at high-affinity sites and how an extended concentration range of Ca^{2+} (50 nM–10 mM) influences this binding. Figure 5A shows that skeletal muscle from membranes isolated from mice of both genotypes bound [^{3}H]Ry in a Ca^{2+}-dependent manner. Despite the fact that Western blotting consistently indicated that skeletal muscle membrane preparations from WT and R163C mice showed no differences in total RyR1 protein expression (Fig. 4, A–C), R163C preparations attained higher [^{3}H]Ry binding levels at Ca^{2+} concentrations ranging from 0.2 to 1000 μM. In the range of Ca^{2+} concentration optimal for [^{3}H]Ry binding, R163C preparations showed ~2-fold higher maximal occu-

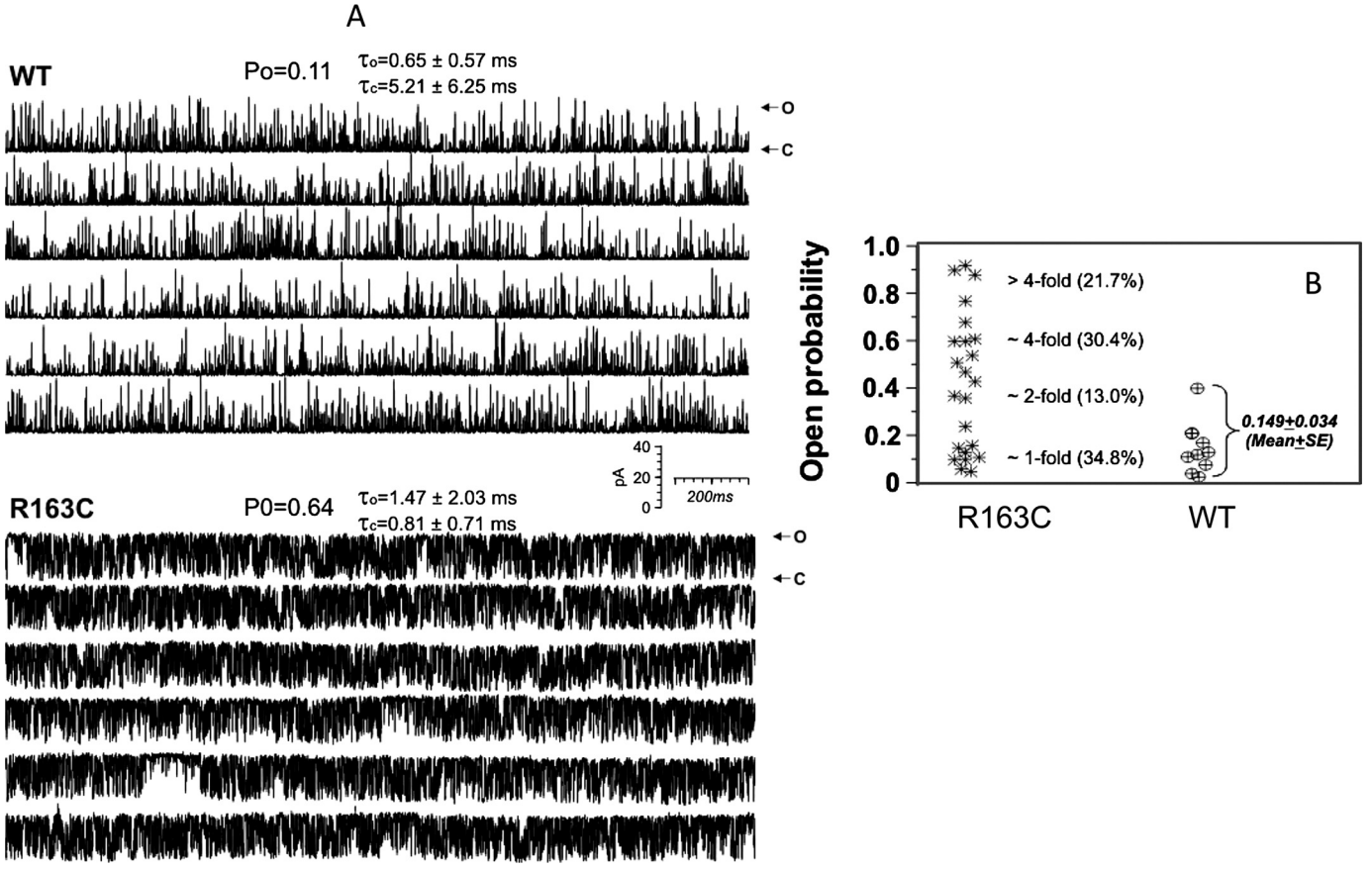

Fig. 5. RyR1 channels reconstituted from R163C preparations have high open probabilities. Single channels were fused with BLM from SR vesicles prepared from either WT or R163C heterozygous mouse skeletal muscles. A, gating behavior of a representative WT channel (top traces) is contrasted with a R163C channel (bottom traces) that exhibited >4-fold higher P_o and was representative of ~22% of the R163C channel reconstituted. The channels were recorded for ≥1 min at −40 mV holding potential applied to *trans*, with *cis* solution (cytosolic) containing 1 μM free (*cis*) Ca^{2+} and 2 mM ATP, and *trans* (luminal) containing 100 μM free Ca^{2+}. P_o was obtained from analysis of individual channel by pClamp 9.0 software. Arrows with o or c indicate the maximal current amplitude when the channel is fully opened or closed, respectively. B, summary of P_o analysis from $n = 9$ WT and $n = 23$ R163C channels recorded under identical experimental conditions. R163C channels exhibiting ≥2-fold P_o compared with WT were statistically significantly at $p < 0.05$ by using unpaired Student's t test. τ_c, mean closed dwell time; τ_o, mean open dwell time.

pancy than WT (Fig. 7A; $n = 8$; $p < 0.0001$). Further analysis revealed that the EC_{50} value for Ca^{2+} activation of [^{3}H]Ry binding to R163C was 3-fold lower than that of WT (EC_{50} = 0.5 ± 0.1 versus 1.6 ± 0.4 μM; $p < 0.01$; Fig. 6B). In contrast, the constant for Ca^{2+} inhibition of [^{3}H]Ry binding (IC_{50}) did not differ between genotypes (331 ± 40 versus 346 ± 31 μM for R163C and WT, respectively (Fig. 7B).

Sensitivity to Mg^{2+} Inhibition Remains Unaltered in R163C. Cytoplasmic Mg^{2+} serves as a physiologically negative modulator of RyR1 channel, restricting channel P_o both under resting and activating conditions (Lamb et al., 2001). Mg^{2+} inhibits RyR1 channel gating at physiological concentrations by competing with Ca^{2+} at both high- and low-affinity sites (Laver et al., 1997a). Several previous studies showed that some MHS mutations reduce the potency of Mg^{2+} as a RyR1 channel inhibitor (Laver et al., 1997b). As expected, Mg^{2+} inhibited [^{3}H]Ry binding to both R163C and WT in a dose-dependent manner (Fig. 7C). Although baseline [^{3}H]Ry binding activity was significantly higher for R163C than that of WT in the absence of Mg^{2+}, binding was completely inhibited by Mg^{2+} ≥5 mM for both genotypes. Further analysis revealed that IC_{50} values did not differ between R163C and WT (410 ± 23 versus 395 ± 28 μM, respectively; Fig. 7D).

R163C Responds to Redox Regulation. In healthy cells, highly reduced cytosolic glutathione redox potentials

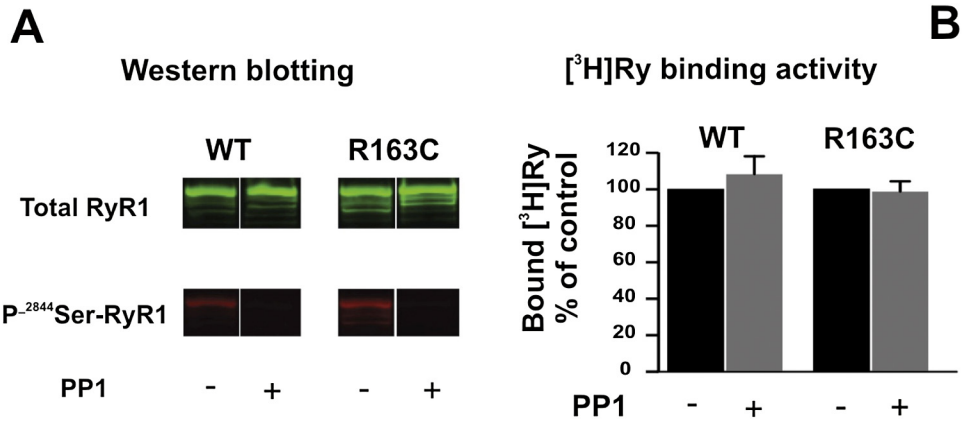

Fig. 6. Dephosphorylation of either R163C RyR1 or WT RyR1 with PP1 has negligible influence on [^{3}H]Ry binding activity. SR from R163C and WT were preincubated with and without PP1 and subsequently analyzed using [^{3}H]Ry binding as described under *Materials and Methods*. A, representative Western blot results (n = 2). B, [^{3}H]Ry binding results (mean ± S.D.) from n = 6 of two paired protein preparations. Statistic analysis indicated no significant difference between the samples pretreated without or with PP1 with preparations from either genotype.

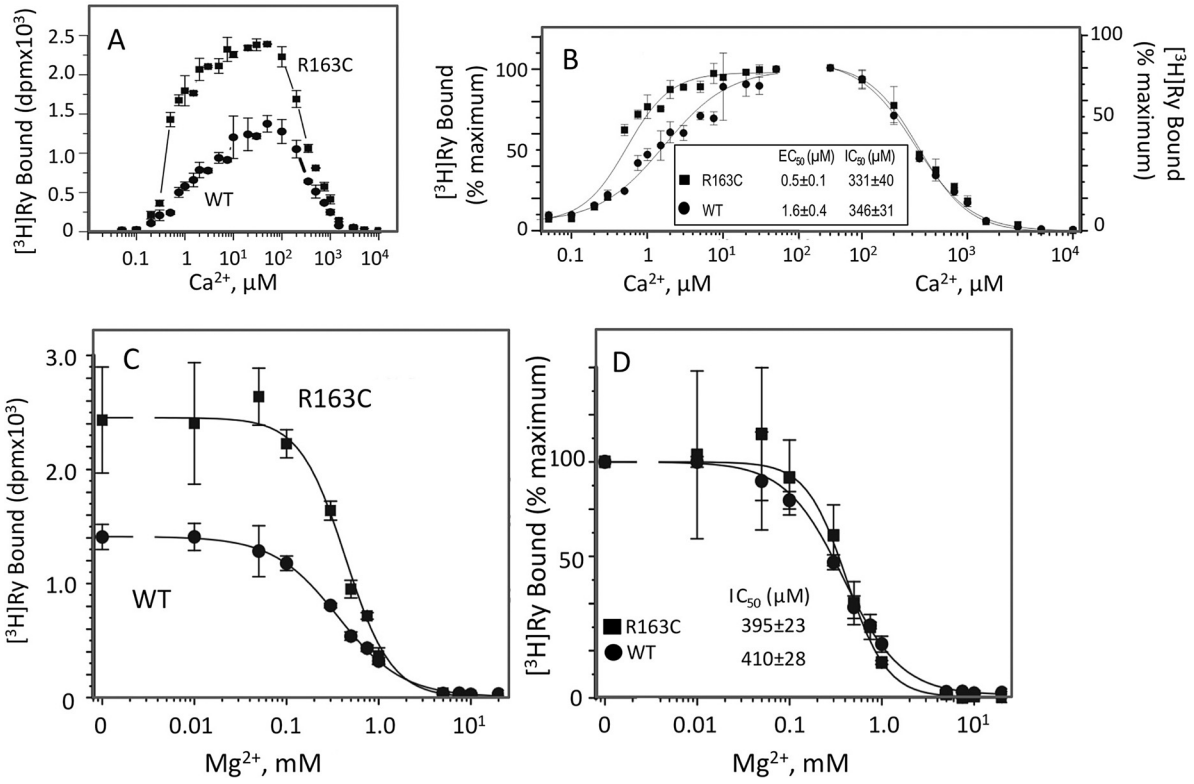

Fig. 7. R163C exhibits altered [^{3}H]Ry binding and Ca^{2+} activation, but inhibition by Ca^{2+} and Mg^{2+} remains unaltered. Equilibrium [^{3}H]ryanodine (2 nM) binding to 100 mg/ml SR protein was performed at 37°C for 3 h in the presence of 50 nM to 10 mM Ca^{2+}. Free Ca^{2+} was adjusted by EGTA according the software Bound and Determined (Voss et al., 2008). The data points are mean ± S.D. from n = 6 determinations from two independent membrane preparations from paired R163C heterozygous and WT mice. A and B, raw data and corresponding data normalized to the maximum binding within each genotype. C and D, Mg^{2+} (0–20 mM) inhibits equilibrium [^{3}H]Ry binding. The free Ca^{2+} in the reaction mixture was buffered by EGTA. The data points are mean ± S.D. from n = 6 determinations from two independent membrane preparations from paired R163C heterozygous and WT mice.

(~220–230 mV) help maintain low RyR1 channel gating activity under resting conditions (Hwang et al., 1995). RyR1 channels are regulated by glutathione redox status, possibly mediated by glutathionylation and/or nitration of hyper-reactive sulfhydryl residues within the channel complex (Marengo et al., 1998; Feng et al., 2000). We assessed how reducing or oxidizing [GSH]/[GSSG] conditions influenced the apparent association rate of [^{3}H]Ry to R163C and WT preparations. Figure 8A shows the initial association of [^{3}H]Ry over the first 15 min of incubation at 37°C in the presence of optimal Ca^{2+} (50 μM) in the assay medium. The bimolecular association (pseudo-first order) rate constants (k_{obs}) were calculated (Fig. 8B). Preparations from R163C mice had significantly faster k_{obs} than those prepared from WT mice when measured in the presence of GSSG (5 mM) (k_{obs} = 19.0 ± 1.9 versus 11.8 ± 1.1 fmol/mg/min, respectively; $p < 0.001$). Although the relative magnitudes of the reduction of [^{3}H]Ry binding rates in an assay medium containing reduced GSH (5 mM) compared with medium containing GSSG were similar in both genotypes (Fig. 8, A and B; ~62.2–67.8%; n = 6–8), the k_{obs} measured in R163C-RyR1 preparations in reducing buffer was nearly identical to the k_{obs} measured with WT-RyR1 in an oxidizing buffer (Fig. 8, A and B). This suggests that the R163C channels are inherently hyperactive, even in the presence of a highly reducing [GSH]/[GSSG] buffer.

To further test whether R163C maintains responses to redox regulation, we focused our comparison on reconstituted R163C channels that possessed P_o >3-fold of WT under standard buffer conditions (*cis*, 1 μM Ca^{2+}, 2 mM ATP/*trans*, 100 μM Ca^{2+}) with undefined *cis/trans* redox potential (no GSH or GSSG added to the solutions). Analysis of n = 6 R163C independent single-channel experiments showed that channels with this mutation maintained a significantly higher mean P_o compared with WT in the presence of a highly reducing [GSH]/[GSSG] potential on the cytoplasmic side (Fig. 8C, *, p = 0.024; left y-axis). However, both R163C and WT channels responded with a similar reduction in P_o once transmembrane redox potential was adjusted to a reducing [GSH]/[GSSG] potential on the cytoplasmic side relative to their respective baseline period (in an undefined redox potential) (Fig. 8C, p = 0.149; right y-axis). Collectively, these results indicate that R163C channels remain responsive to changes in *cis* redox potential but maintain significantly higher P_o than WT channels even under highly reducing redox potential, indicating that channels with the R163C mutation are inherently hyperactive.

Influence of Temperature on [^{3}H]Ry Binding Kinetics. Because temperature may be a critical factor in triggering MH in susceptible individuals, we compared the apparent rate (k_{obs}) of [^{3}H]Ry binding at two temperatures, 25 and 37°C. Figure 9 shows that as expected k_{obs} was significantly

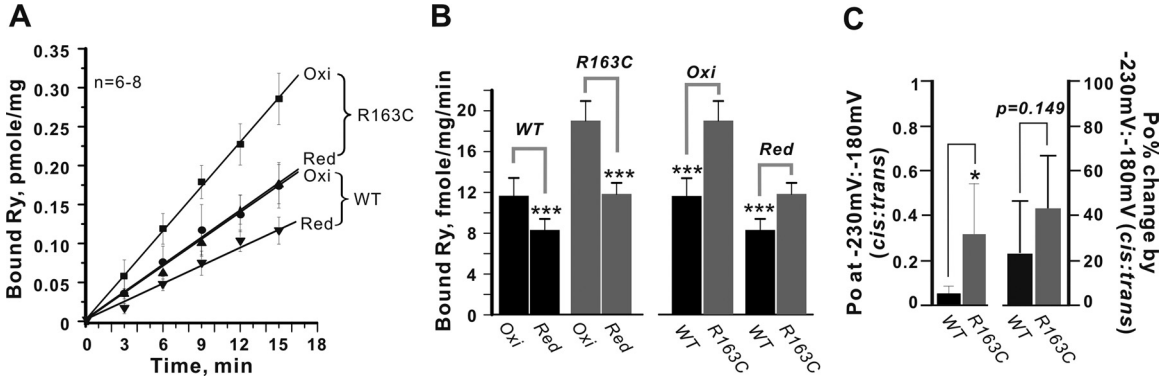

Fig. 8. Response of R163C channels to glutathione redox potential. Reducing (Red) and oxidizing (Oxi) conditions were set in the assay buffer by addition of 5 mM GSH and 5 mM GSSG, respectively. [^{3}H]Ry (5 nM) was added to the assay buffer to initiate the binding, and the reaction quenched at the indicated time points by filtration. The binding reaction was terminated at 0, 3, 6, 9, 12, 15 min, and the results are plotted in A. The pseudo-first order binding rates (k_{obs}) were obtained from the linear fitting and plotted as bar graphs in B (n = 6–8 determinations). C, summarizes analysis of single-channel P_o in the presence of a transmembrane redox potential set at −230 mV/−180 mV (*cis/trans*) for n = 6 independent R163C and WT channels reconstituted in BLM (left y-axis label). The respective changes in P_o when the transmembrane redox potential were set at −230 mV/−180 mV (*cis/trans*) relative to the corresponding control period for WT (n = 6) and R163C (n = 6) channels are shown (right y-*axis* label). Mean± S.D. are shown and were not statistically different between the two genotypes (p = 0.149). Statistical analyses indicate where significant differences were found using independent Student's t tests (*, $p < 0.05$; ***, $p < 0.001$).

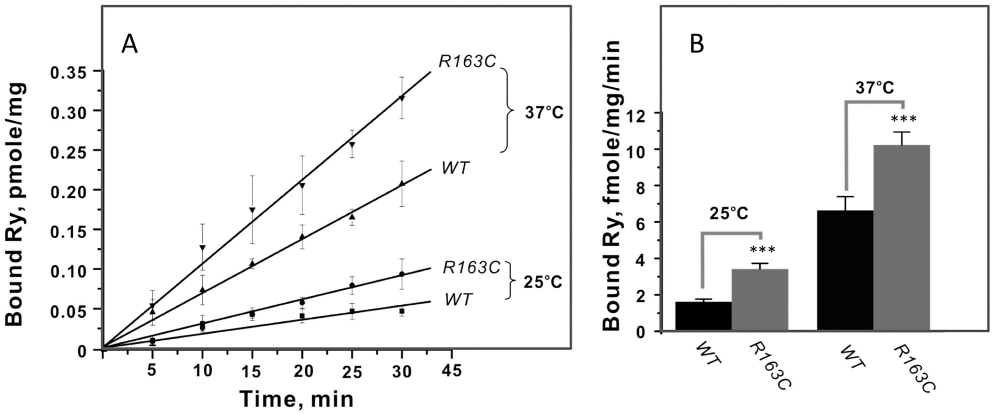

Fig. 9. Influence of temperature on [^{3}H]Ry binding kinetics to R163C and WT preparations. Binding of 5 nM [^{3}H]Ry to 100 μg/ml SR preparations was initiated at either 25 or 37°C and quenched at 5, 10, 15, 20, 25, and 30 min. The rate lines are plotted (A). The initial rates were obtained from linear curve fitting (B), and the calculated k_{obs} values are plotted as bar graphs (A). Statistical analyses indicate significant difference among the compared groups (***, $p < 0.001$; n = 6–8).

slower at 25°C than at 37°C for both heterozygous R193C and WT genotypes. Interestingly the k_{obs} for R163C was 1.5-fold faster at 37°C and 2-fold faster at 25°C compared with the k_{obs} values obtained from WT at the respective temperatures.

Discussion

The R163C mutation is one of the five most common mutations conferring MHS in humans (Robinson et al., 2006). This study identifies several impairments inherent to the regulation of R163C RyR1 isolated from skeletal muscle of heterozygous mice in the absence of triggering agents. Most notable is the significantly higher single-channel activity exhibited by R163C compared with WT. If one assumes that RyR1 monomers composed of WT and R163C gene products randomly associate to form functional channel tetramers, then five distinct combinations of WT and R163C monomers could contribute to divergent channel gating behaviors in BLM experiments with SR prepared from heterozygous R163C. In fact, ~35% of the R163C channels reconstituted in BLM were found to possess open probabilities not significantly different from those measured for channels prepared from WT skeletal muscle under the defined experimental conditions used in this study. The remaining 65% of the channels measured had 2- to >4-fold higher P_o values ($p < 0.05$) than WT. This distribution of P_o values suggests that a ratio of 1 R163C:3 WT monomers within a channel tetramer may alter channel P_o in a subtle manner difficult to resolve given the limitations of the BLM method. Nevertheless, the divergence of P_o values observed in 65% of the channels recorded may reflect a gene-dose effect, with tetramers composed of 2:2, 3:1, and 4:0 ratios of R163C:WT monomers increasing the probability of transitions to the channel open state.

Because of birth lethality in R163C homozygous mice, this hypothesis could not be directly tested in SR prepared from adult skeletal muscle. Binding studies with [^{3}H]Ry indicate that membranes prepared from R163C mice bind significantly more (2-fold) radioligand in the presence of an optimal Ca^{2+} buffer compared with WT. This difference in occupancy is not a result of differential expression of protein in R163C preparations, because the levels of RyR1-immunoreactive protein did not differ between the genotypes when measured in the same preparations used for binding analysis. Collectively, these data indicate that the majority of R163C channels recovered from heterozygous mice have inherently higher activity than WT.

A possible contributor leading to enhanced channel activity was the significantly higher levels of phosphorylation at ^{2844}Ser observed with R163C-RyR1. Phosphorylation of RyR1 destabilized interactions with FKBP12 and was associated enhanced channel activity (Reiken et al., 2003) and promoted RyR1 channel substrate behavior (Marx et al., 2000). Thus, one possible mechanism that may contribute to destabilization of the closed state of R163C channels is the loss of FKBP12, even in the absence of triggering agents.

However, our results with R163C-RyR1 do not support this hypothesis because the ratio of FKBP12/RyR1 did not differ in heavy SR preparations from R163C and WT. Moreover, R163C channels remained responsive to bastadin 5 ($n = 4$ of four R163C-RyR1 channels; W. Feng, unpublished observation), a compound known to activate RyR1 channel in FKBP12-dependent manner (Mack et al., 1994). Dephosphorylation of RyR1 with exogenous PP1 had little effect on [^{3}H]Ry binding to either genotype, despite the near-complete loss of signal using the phospho-^{2488}Ser-RyR1 antibody. Furthermore, PP1 added to RyR1 preparations before or after single channels were reconstituted in BLM failed to reduce the channel P_o of either WT or R163C preparations in continuous recordings lasting 20 to 60 min (W. Feng, unpublished data). Thus increased phosphorylation of R163C-RyR1 compared with WT under basal conditions (i.e., in the absence of triggering agent) has little influence on the amount of FKBP12 associated and therefore cannot directly account for the pronounced differences in channel behavior observed between these genotypes. Although ours is the first evidence that the phosphorylation level at ^{2844}Ser-RyR1 is not associated with impaired binding of FKBP12, a similar conclusion was reached based on the lack of measurable effect of protein kinase A-dependent RyR2 phosphorylation on binding of either FKBP12 or −12.6 in cardiomyocytes (Guo et al., 2010).

Heightened sensitivity to activation by cytoplasmic Ca^{2+} is the prominent characteristic of R163C channels, even under highly reducing redox potentials, and it may reflect a lowered energy barrier needed for opening the channel and unmasking high-affinity binding sites for ryanodine. Although high-affinity binding of [^{3}H]Ry and channel activity are low when cytoplasmic Ca^{2+} is adjusted to ≤100 nM, R163C myotubes and adult fast twitch fibers maintain a chronically elevated $[Ca^{2+}]_{rest}$. Therefore, at resting condition, when $[Ca^{2+}]_{rest}$ is >200 nM, the influence of R163C on high-conductance channel gating would be most pronounced during Ca^{2+} release triggered by EC coupling as Ca^{2+} on the cytoplasmic face of the channel increases. Expression of RyR1 is responsible for more than half of the total $[Ca^{2+}]_{rest}$ measured in WT myotubes (Eltit et al., 2010); compared with WT, MHS mutations significantly raise $[Ca^{2+}]_{rest}$ (Yang et al., 2007b) that may arise from the RyR1 ryanodine-insensitive Ca^{2+} leak conformation (Pessah et al., 1997). Thus, altered regulation of R163C by Ca^{2+} is likely to contribute to the pronounced destabilizing effects of agents that trigger MH. Contrary to previous results obtained from [^{3}H]Ry binding and single-channel analyses of SR prepared from homozygous porcine R615C (Balog et al., 2001) and R163C expressed in 1B5 RyR-null myotubes (Yang et al., 2006), we did not find significant shifts in either inhibition by Mg^{2+} or high Ca^{2+} compared with WT. Whether the divergence reflects zygosity, the penetrance of the two mutations, species differences, or a combination remains unclear.

The higher sensitivity of R163C channels to Ca^{2+} and the inability of physiological reducing potentials to restore the low P_o gating state seen in WT suggest that R163C channels possessing R163C mutation(s) are inherently hyperactive. Channel hyperactivity could be the consequence of complex mechanisms that involve glutathionylation and nitrosylation of RyR1 at reactive cysteines (Durham et al., 2008), but it does not seem to be a direct consequence of increased phosphorylation. The allosteric structural changes caused by the R163C mutation could promote formation and stabilize inappropriate disulfide bond(s) with reactive cysteine normally present in RyR1 (Feng et al., 2000; Voss et al., 2004) and/or disrupt intra- or intersubunit interactions (Tung et al., 2010). Here, we did not discriminate which of these mechanisms contributes to channel dysfunction. Nevertheless, because

triggering fulminant MH is associated with oxidative bursts, ineffective regulation of R163C channels by glutathione may not only contribute to uncontrolled release of SR Ca^{2+} but also further promote it.

To our knowledge, the present study is the first to examine how functional dysregulation of a common heterozygous MHS mutation influences EC coupling behavior in intact myotubes and adult skeletal muscle fibers derived from the same animals. R163C has a clearly observable influence on EC coupling in myotubes but not in adult FDB fibers. Significantly depressed Ca^{2+} transient amplitudes observed at all stimulus frequencies (1–60 Hz) is consistent with the recent report of Bannister et al. (2010) using voltage clamp of R163C and WT myotubes. The reduced amplitudes elicited by electrical stimuli seen with R163C could result from partial depletion of SR Ca^{2+} stores conferred by MHS SR that is chronically more leaky to Ca^{2+} than WT in the affected myotubes (Bannister et al., 2010). We reported previously that ECCE in R163C myotubes was significantly enhanced compared with that in WT (Cherednichenko et al., 2008). Here, we extend these findings over a broad range of stimulus frequencies, and we report that although enhanced ECCE occurs at stimuli ≤20 Hz, at higher frequencies ECCE begins to fail and is associated with failure to maintain the Ca^{2+} transient amplitude during a 10-s, 60-Hz pulse train. One possible contributor to the failure of ECCE at high frequencies may be related to the delay in the inactivation process (Bannister et al., 2010). The present study supports that altered bidirectional signaling between DHPR and RyR1 contributes to the MHS phenotype.

An unexpected observation is that Ca^{2+} transient amplitudes measured in heterozygous R163C FDB fibers do not differ from their WT counterpart in the stimulus range tested, consistent with contractility measurements made at 25°C with soleus fibers isolated from heterozygous Y522S and WT mice (Chelu et al., 2006). Our analyses of [^{3}H]Ry binding show a significantly greater k_{obs} (pseudo-first order rate) for R163C at either 25 or 37°C, indicating inherent channel dysfunction occurs at lower than physiological temperatures.

Perhaps the lack of a detectible impairment in the Ca^{2+} transient phenotype of FDB fibers when assayed under basal conditions should not be considered unexpected, given that heterozygous R163C mice do not exhibit an overt phenotype throughout their life span in the absence of temperature stress or triggering agent. One possible explanation for the divergence in EC-coupling deficit seen in myotubes and adult FDB fibers from heterozygous R163C mice is that adult fibers have more developed Ca^{2+} release units than myotubes (Flucher and Franzini-Armstrong, 1996). Moreover, myotubes express RyR1 splice variants not found in adult fibers that magnify depolarization-dependent Ca^{2+} release (Kimura et al., 2009). Alternatively, myotubes express a high-conductance $\alpha 1$ $Cav_{1.1}$ isoform not found in adult fibers (Tuluc et al., 2009). The rather remarkable dysfunction of R163C channels measured from SR preparations prepared from adult mice must be limited by strong negative regulation in context of the Ca^{2+} release unit of adult fibers, and to a lesser extent, in myotubes where the junctions are less developed and have different CRU composition. This hypothesis is consistent with previous data that identifies the DHPR as a strong negative regulatory module of RyR1 (Zhou et al., 2006). This possibility could explain the pharmacogenic nature of MH; a lack of overt phenotype under basal physiological circumstances despite the presence of inherently dysregulated RyR1 channels. The rapid appearance of fulminant life-threatening MH in response to temperature stress and triggering agents could be mediated by weakening of the negative feedback provided by DHPR, thereby unmasking the full dysfunction of MHS RyR1. This hypothesis deserves investigation.

Authorship Contributions

Participated in research design: Feng, Barrientos, Cherednichenko, and Pessah.

Conducted experiments: Feng, Barrientos, Cherednichenko, Padilla, Truong, and Lopez.

Contributed new reagents or analytic tools: Yang and Allen.

Performed data analysis: Feng, Barrientos, Cherednichenko, Padilla, Truong, Lopez, and Pessah.

Wrote or contributed to the writing of the manuscript: Feng, Barrientos, Cherednichenko, Allen, and Pessah.

References

Airey JA, Beck CF, Murakami K, Tanksley SJ, Deerinck TJ, Ellisman MH, and Sutko JL (1990) Identification and localization of two triad junctional foot protein isoforms in mature avian fast twitch skeletal muscle. *J Biol Chem* **265:**14187–14194.

Balog EM, Fruen BR, Shomer NH, and Louis CF (2001) Divergent effects of the malignant hyperthermia-susceptible Arg(615)→Cys mutation on the Ca(2+) and Mg(2+) dependence of the RyR1. *Biophys J* **81:**2050–2058.

Bannister RA, Estève E, Eltit JM, Pessah IN, Allen PD, López JR, and Beam KG (2010) A malignant hyperthermia-inducing mutation in RYR1 (R163C): consequent alterations in the functional properties of DHPR channels. *J Gen Physiol* **135:**629–640.

Brown LD, Rodney GG, Hernández-Ochoa E, Ward CW, and Schneider MF (2007) Ca^{2+} sparks and T tubule reorganization in dedifferentiating adult mouse skeletal muscle fibers. *Am J Physiol Cell Physiol* **292:**C1156–C1166.

Buck ED, Nguyen HT, Pessah IN, and Allen PD (1997) Dyspedic mouse skeletal muscle expresses major elements of the triadic junction but lacks detectable ryanodine receptor protein and function. *J Biol Chem* **272:**7360–7367.

Chelu MG, Goonasekera SA, Durham WJ, Tang W, Lueck JD, Riehl J, Pessah IN, Zhang P, Bhattacharjee MB, Dirksen RT, et al. (2006) Heat- and anesthesia-induced malignant hyperthermia in an RyR1 knock-in mouse. *FASEB J* **20:**329–330.

Cherednichenko G, Hurne AM, Fessenden JD, Lee EH, Allen PD, Beam KG, and Pessah IN (2004) Conformational activation of Ca^{2+} entry by depolarization of skeletal myotubes. *Proc Natl Acad Sci USA* **101:**15793–15798.

Cherednichenko G, Ward CW, Feng W, Cabrales E, Michaelson L, Samso M, López JR, Allen PD, and Pessah IN (2008) Enhanced excitation-coupled calcium entry in myotubes expressing malignant hyperthermia mutation R163C is attenuated by dantrolene. *Mol Pharmacol* **73:**1203–1212.

Durham WJ, Aracena-Parks P, Long C, Rossi AE, Goonasekera SA, Boncompagni S, Galvan DL, Gilman CP, Baker MR, Shirokova N, et al. (2008) RyR1 S-nitrosylation underlies environmental heat stroke and sudden death in Y522S RyR1 knockin mice. *Cell* **133:**53–65.

Eltit JM, Yang T, Li H, Molinski TF, Pessah IN, Allen PD, and Lopez JR (2010) RyR1-mediated Ca^{2+} leak and Ca^{2+} entry determine resting intracellular Ca^{2+} in skeletal myotubes. *J Biol Chem* **285:**13781–13787.

Estève E, Eltit JM, Bannister RA, Liu K, Pessah IN, Beam KG, Allen PD, and López JR (2010) A malignant hyperthermia-inducing mutation in RYR1 (R163C): alterations in Ca^{2+} entry, release, and retrograde signaling to the DHPR. *J Gen Physiol* **135:**619–628.

Feng W, Liu G, Allen PD, and Pessah IN (2000) Transmembrane redox sensor of ryanodine receptor complex. *J Biol Chem* **275:**35902–35907.

Flucher BE and Franzini-Armstrong C (1996) Formation of junctions involved in excitation-contraction coupling in skeletal and cardiac muscle. *Proc Natl Acad Sci USA* **93:**8101–8106.

Guo T, Cornea RL, Huke S, Camors E, Yang Y, Picht E, Fruen BR, and Bers DM (2010) Kinetics of FKBP12.6 binding to ryanodine receptors in permeabilized cardiac myocytes and effects on Ca sparks. *Circ Res* **106:**1743–1752.

Hwang C, Lodish HF, and Sinskey AJ (1995) Measurement of glutathione redox state in cytosol and secretory pathway of cultured cells. *Methods Enzymol* **251:**212–221.

Kimura T, Lueck JD, Harvey PJ, Pace SM, Ikemoto N, Casarotto MG, Dirksen RT, and Dulhunty AF (2009) Alternative splicing of RyR1 alters the efficacy of skeletal EC coupling. *Cell Calcium* **45:**264–274.

Lamb GD, Posterino GS, Yamamoto T, and Ikemoto N (2001) Effects of a domain peptide of the ryanodine receptor on Ca^{2+} release in skinned skeletal muscle fibers. *Am J Physiol Cell Physiol* **281:**C207–C214.

Laver DR, Baynes TM, and Dulhunty AF (1997a) Magnesium inhibition of ryanod-

ine-receptor calcium channels: evidence for two independent mechanisms. *J Membr Biol* **156:**213–229.
Laver DR, Owen VJ, Junankar PR, Taske NL, Dulhunty AF, and Lamb GD (1997b) Reduced inhibitory effect of Mg^{2+} on ryanodine receptor-Ca^{2+} release channels in malignant hyperthermia. *Biophys J* **73:**1913–1924.
Lehmann-Horn F, Jurkat-Rott K, Rüdel R, and Ulm Muscle Centre (2008) Diagnostics and therapy of muscle channelopathies—guidelines of the Ulm Muscle Centre. *Acta Myol* **27:**98–113.
Mack MM, Molinski TF, Buck ED, and Pessah IN (1994) Novel modulators of skeletal muscle FKBP12/calcium channel complex from *Ianthella basta*: role of FKBP12 in channel gating. *J Biol Chem* **269:**23236–23249.
Marengo JJ, Hidalgo C, and Bull R (1998) Sulfhydryl oxidation modifies the calcium dependence of ryanodine-sensitive calcium channels of excitable cells. *Biophys J* **74:**1263–1277.
Marx SO, Reiken S, Hisamatsu Y, Jayaraman T, Burkhoff D, Rosemblit N, and Marks AR (2000) PKA phosphorylation dissociates FKBP12.6 from the calcium release channel (ryanodine receptor): defective regulation in failing hearts. *Cell* **101:**365–376.
Pessah IN, Molinski TF, Meloy TD, Wong P, Buck ED, Allen PD, Mohr FC, and Mack MM (1997) Bastadins relate ryanodine-sensitive and ryanodine-insensitive "leak" Ca^{2+} efflux pathways in skeletal SR and BC_3H1 cells. *Am J Physiol* **272:**C601–C614.
Protasi F (2002) Structural interaction between RYRs and DHPRs in calcium release units of cardiac and skeletal muscle cells. *Front Biosci* **7:**d650–d658.
Reiken S, Lacampagne A, Zhou H, Kherani A, Lehnart SE, Ward C, Huang F, Gaburjakova M, Gaburjakova J, Rosemblit N, et al. (2003) PKA phosphorylation activates the calcium release channel (ryanodine receptor) in skeletal muscle: defective regulation in heart failure. *J Cell Biol* **160:**919–928.
Robinson R, Carpenter D, Shaw MA, Halsall J, and Hopkins P (2006) Mutations in RYR1 in malignant hyperthermia and central core disease. *Hum Mutat* **27:**977–989.
Robinson RL, Anetseder MJ, Brancadoro V, van Broekhoven C, Carsana A, Censier K, Fortunato G, Girard T, Heytens L, Hopkins PM, et al. (2003) Recent advances in the diagnosis of malignant hyperthermia susceptibility: how confident can we be of genetic testing? *Eur J Hum Genet* **11:**342–348.
Sheridan DC, Takekura H, Franzini-Armstrong C, Beam KG, Allen PD, and Perez CF (2006) Bidirectional signaling between calcium channels of skeletal muscle requires multiple direct and indirect interactions. *Proc Natl Acad Sci USA* **103:**19760–19765.
Ta TA, Feng W, Molinski TF, and Pessah IN (2006) Hydroxylated xestospongins block inositol-1,4,5-trisphosphate-induced Ca^{2+} release and sensitize Ca^{2+}-induced Ca^{2+} release mediated by ryanodine receptors. *Mol Pharmacol* **69:**532–538.
Takeshima H, Iino M, Takekura H, Nishi M, Kuno J, Minowa O, Takano H, and Noda T (1994) Excitation-contraction uncoupling and muscular degeneration in mice lacking functional skeletal muscle ryanodine-receptor gene. *Nature* **369:**556–559.
Tuluc P, Molenda N, Schlick B, Obermair GJ, Flucher BE, and Jurkat-Rott K (2009) A CaV1.1 Ca^{2+} channel splice variant with high conductance and voltage-sensitivity alters EC coupling in developing skeletal muscle. *Biophys J* **96:**35–44.
Tung CC, Lobo PA, Kimlicka L, and Van Petegem F (2010) The amino-terminal disease hotspot of ryanodine receptors forms a cytoplasmic vestibule. *Nature* **468:**585–588.
Voss AA, Allen PD, Pessah IN, and Perez CF (2008) Allosterically coupled calcium and magnesium binding sites are unmasked by ryanodine receptor chimeras. *Biochem Biophys Res Commun* **366:**988–993.
Voss AA, Lango J, Ernst-Russell M, Morin D, and Pessah IN (2004) Identification of hyperreactive cysteines within ryanodine receptor type 1 by mass spectrometry. *J Biol Chem* **279:**34514–34520.
Yang T, Allen PD, Pessah IN, and Lopez JR (2007a) Enhanced excitation-coupled calcium entry in myotubes is associated with expression of RyR1 malignant hyperthermia mutations. *J Biol Chem* **282:**37471–37478.
Yang T, Esteve E, Pessah IN, Molinski TF, Allen PD, and López JR (2007b) Elevated resting [Ca(2+)](i) in myotubes expressing malignant hyperthermia RyR1 cDNAs is partially restored by modulation of passive calcium leak from the SR. *Am J Physiol Cell Physiol* **292:**C1591–C1598.
Yang T, Riehl J, Esteve E, Matthaei KI, Goth S, Allen PD, Pessah IN, and Lopez JR (2006) Pharmacologic and functional characterization of malignant hyperthermia in the R163C RyR1 knock-in mouse. *Anesthesiology* **105:**1164–1175.
Zhou J, Allen PD, Pessah IN, and Naguib M (2010) Neuromuscular disorders and malignant hyperthermia, in *Miller's Anesthesia* (Miller RD ed) p 1171, Churchill Livingstone, Philadelphia.
Zhou J, Yi J, Royer L, Launikonis BS, González A, García J, and Ríos E (2006) A probable role of dihydropyridine receptors in repression of Ca^{2+} sparks demonstrated in cultured mammalian muscle. *Am J Physiol Cell Physiol* **290:**C539–C553.

Address correspondence to: Dr. Isaac N. Pessah, Department of Molecular Biosciences, School of Veterinary Medicine, One Shields Ave., University of California, Davis, CA 95616. E-mail: inpessah@ucdavis.edu